

522373



Sandia National Laboratories

Operated for the U.S. Department of Energy by

Sandia Corporation

P.O. Box 5800
Albuquerque, NM 87185-1395

Phone: (505) 234-0110 (Carlsbad)
Phone: (505) 845-0936 (Abq Direct Line)
Fax: (505) 234-0081
Internet: jsstein@sandia.gov

Joshua S. Stein 5/20/2002

Joshua S. Stein Ph. D.
Performance Assessment & Decision Analysis Department
4100 National Parks Hwy., Carlsbad, NM 88220

date: 13 May 2002

to: Kathryn Knowles, 06821
Performance Assessment and Decision Analysis

from: Joshua S. Stein (SNL, Org 6821)

subject: Methodology behind the TBM BRAGFLO grid.

1.0 INTRODUCTION AND OBJECTIVES

This memo describes the methodology used to create the two-dimensional BRAGFLO computational grid used for the Technical Baseline Migration (TBM) calculations. The TBM is an effort to merge CCA (U.S. DOE, 1996) and PAVT (PAVT, 1997) baselines while at the same time implementing conceptual model changes being reviewed by the Conceptual Models Peer Review Panel, May 2002. The TBM grid is similar to the baseline grid that was used for the CCA and PAVT, except for the differences that are described below. (Note: Stein (2002) describes details of the Salado flow calculations for the TBM).

The most important changes with respect to the TBM BRAGFLO grid are the removal of the shaft seal system and the implementation of the Option D panel closures. Additional grid refinements have also been implemented to increase numerical accuracy and computational efficiency, and reduce numerical dispersion, but these refinements do not entail any changes to conceptual models. For completeness all changes are described here. Attached to this memo is an Excel spreadsheet where the grid cell dimensions are calculated.

2.0 APPROACH

The baseline grid used in the CCA & PAVT had (NX, NY) dimensions of (33, 31). The new grid for the TBM has dimensions (68, 33). The specific changes that were implemented in the TBM grid are listed below and then discussed in more detail in the following sections. Logical grids for the baseline and TBM are shown at the end of the memo.

List of changes implemented in the TBM Grid:

1. Shaft is removed.
2. Option D type panel closures are implemented.
3. Segmentation of the waste regions is increased.

Exceptional Service in the National Interest

WIPP: 1.3.5.2.1.1 Q A: DPRPI: 520523

4. Grid flaring method is redefined and simplified.
5. *X* spacing of the grid beyond the repository to the north and south is refined.
6. Layers above and below Marker Bed 139 have been made relatively thin (~1 m thick) and *Y*-spacing in Salado has been changed.

2.1 Removal of the shaft from the BRAGFLO grid

The baseline grid included a composite shaft representing the combination of the four repository shafts and their associated surrounding DRZ. Deterministic numerical modeling in support of the shaft seal design demonstrated that the shaft seal design is exceedingly effective in preventing flow up the shaft (CCA, Appendix SEAL). In addition, all PA calculations have resulted in negligible flow up the shaft and in no vector was the shaft seal system a pathway for releases (Helton et al., 1998; PAVT, 1997). For these reasons we are proposing to screen this release pathway out of the analysis and remove this component from the model domain.

Removal of the shaft from the grid has beneficial numerical modeling consequences. The shaft's presence had an unrealistic influence on units above the repository by blocking horizontal flow between regions separated by the shaft; in reality, these regions communicate around the shaft materials. In addition, the shaft required over 400 parameters to be implemented into the PA calculations. Its removal, makes model set-up and calculation debugging more transparent.

2.2 Implementation of Option D type panel closures.

In the CCA, the Department of Energy (DOE) presented four options for panel closure designs (A-D). Upon reviewing the CCA, the Environmental Protection Agency (EPA) mandated the implementation of the Option D design, which should provide the tightest closure between panels. For the TBM we implement the cross-sectional area of the Option D panel closures parallel to flow. In addition, to appropriately represent the effect of Option D geometry on repository fluid flow, the segmentation of the waste regions was increased in the grid. This change is described fully in §2.3.

For the TBM, four sets of panel closures were included in the model domain. The southernmost set of closures represents a pair of closures separating a single panel from the other waste areas. The three other sets of closures represent the three sets of 4 panel closures intended for 1) the middle of the waste area, 2) between the waste area and the operations area, and 3) between the operations area and the shafts.

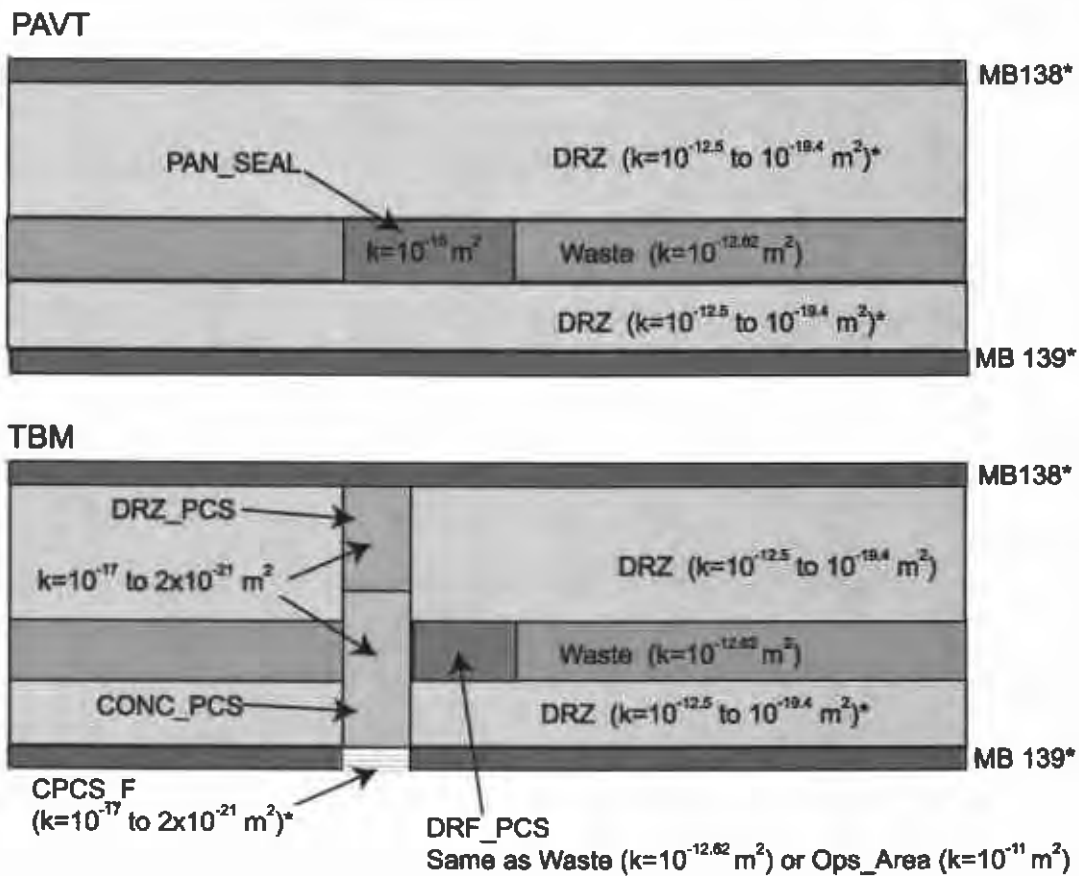
Each set of panel closures is represented in the TBM grid with 4 materials (Stein, 2002). Refer to Figure 1.

1. CONC_PCS: material representing Salado Mass Concrete (SMC).
2. DRZ_PCS: material representing healed DRZ.
3. DRF_PCS: material representing the empty drift + explosion wall. The material is treated as WAS_AREA (but is not filled with waste) for the three panel closures that are adjacent to waste regions, and as OPS_AREA for the single closure between the OPS_AREA and the EXP_AREA. This is done so that the creep closure model is applied consistently to different regions in the grid (WAS_AREA has the creep closure model applied whereas OPS_AREA is pre-closed and assigned an initial low porosity for all times).

- CPCS_F: material representing SMC at low pressures but which is allowed to fracture at high pressures similar to the anhydrite Marker Bed 139 located the same level. The application of the fracture model simulates a fluid pathway around the panel closure in the event that fracture pressures are reached. Such a pathway is reasonable because floor heave will cause fracturing of the lower DRZ, establishing a hydraulic path to Marker Bed 139.

Figure 1 is a schematic diagram comparing the panel closure implementation in the baseline and TBM grids. Permeability ranges are indicated for all materials.

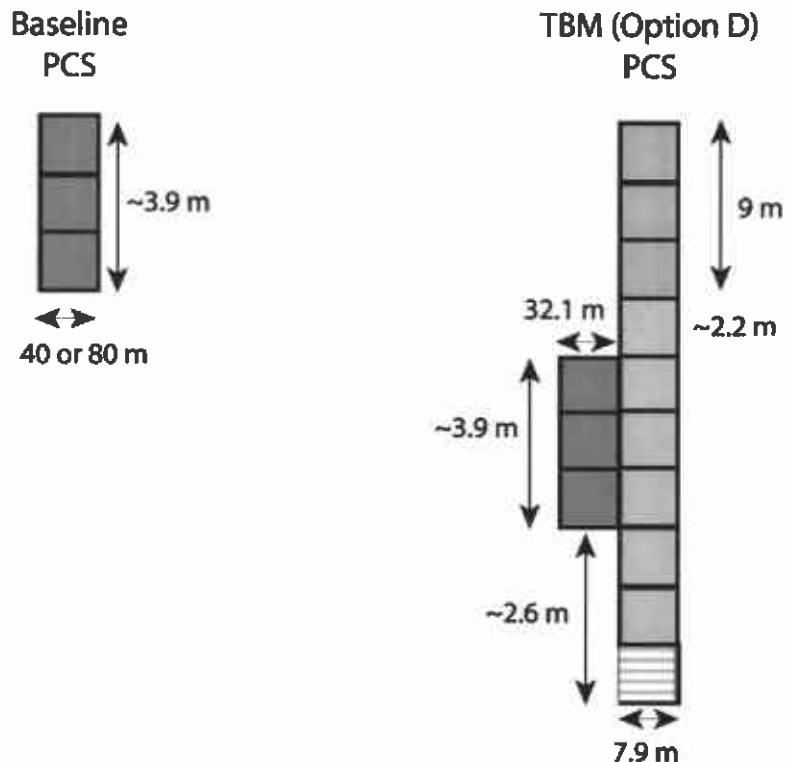
Figure 1.



[* = allowed to fracture, permeability is pressure dependant above ~12.5 MPa]

Each set of panel closures is represented by 13 cells in the TBM BRAGFLO grid, as shown below in Figure 2.

Figure 2.

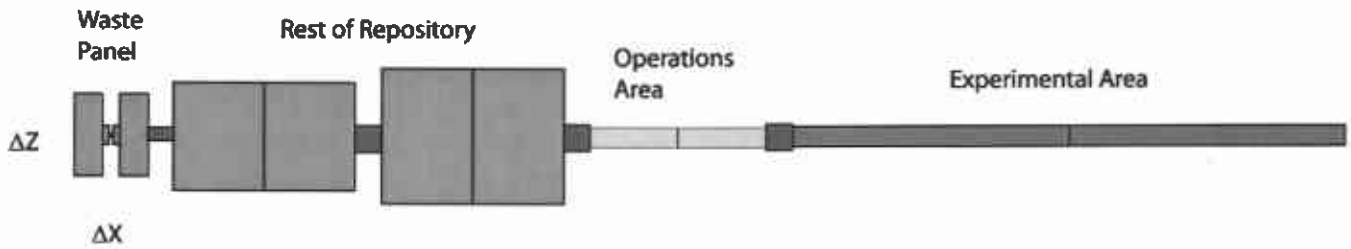


2.3 Increased segmentation of waste regions in grid.

The baseline grid divided the waste regions into two regions, the Intruded or Waste Panel (IP) and the Rest of Repository (RoR). The IP represented a single waste panel located in the southern end of the repository. The RoR represented the other nine panels. Because the effect of Option D panel closures is expected to impede flow between panels it was necessary to divide the RoR into northern and southern blocks separated by a set of panel closures. This change more accurately represents the effect of impeded flow between panels, especially after an intrusion event, which only occurs in the Intruded Panel. To implement this change and allow for the representations of additional panel closures the X-extents and locations of the rest of repository blocks changed. The delta Z dimensions of these blocks were chosen so that the volume of the total RoR matched that in the baseline grid.

Figure 3 shows a scaled view of the repository portion of the TBM grid looking from above.

Figure 3.



2.4 Redefined and simplified grid flaring method.

Grid flaring is a method to represent 3-D volumes in a 2-D grid. Flaring is used when flows can be represented as divergent and convergent from the center of flaring. The baseline grid used flaring at two different scales: locally around the borehole and shaft, and regionally around a point in the northern end of the RoR. For the TBM we do not change the local flaring around the borehole. We eliminate flaring associated with the shaft, since it has been removed, and we redefine and simplify the way in which the regional flaring is calculated.

The regional rectangular flaring occurs *only* for the grid blocks to the north and south of the excavated region. The flaring is similar to what was done for the baseline grid, however the exact flaring configuration is not adequately documented for the baseline grid. The flaring method used for the TBM grid is similar to what was done for the baseline grid but simpler (Figure 4). Looking from the top of the grid (x - z plane), consider that the excavated region is now represented by a rectangle of length $x = 1830$ m and width $z = 80$ m, we call this East-West distance, D_{EW} . This simplification maintains the area (and volume) of the actual gridded excavated region for the calculation of the Δz 's needed to represent flaring. In order to calculate the rectangular flaring we define a centerline to divide the flaring on the north and south. Because the waste panels are located in the southern part of the excavated area, we choose the centerline to be the "center of waste" as the middle of the PCS that separates the northern RoR from the southern RoR. We describe the position of this "center of the waste" by the distances from the north and south edges of the gridded repository, D_N and D_S , respectively. $\{D_N = 1378$ m, $D_S = 452$ m, $D_N + D_S = 1830$ m $\}$ Each flared grid block has length, Δx , and width, Δz . The block can be thought of as wrapped around the excavated area like half a rectangular onion, with the center at the center of waste (Figure 4). Each Δz can be calculated from the preceding Δx 's as follows.

For the northern end:

$$\Delta z_1 = 2D_N + D_{EW} + 2\Delta x_1$$

$$\Delta z_2 = 2D_N + D_{EW} + 4\Delta x_1 + 2\Delta x_2$$

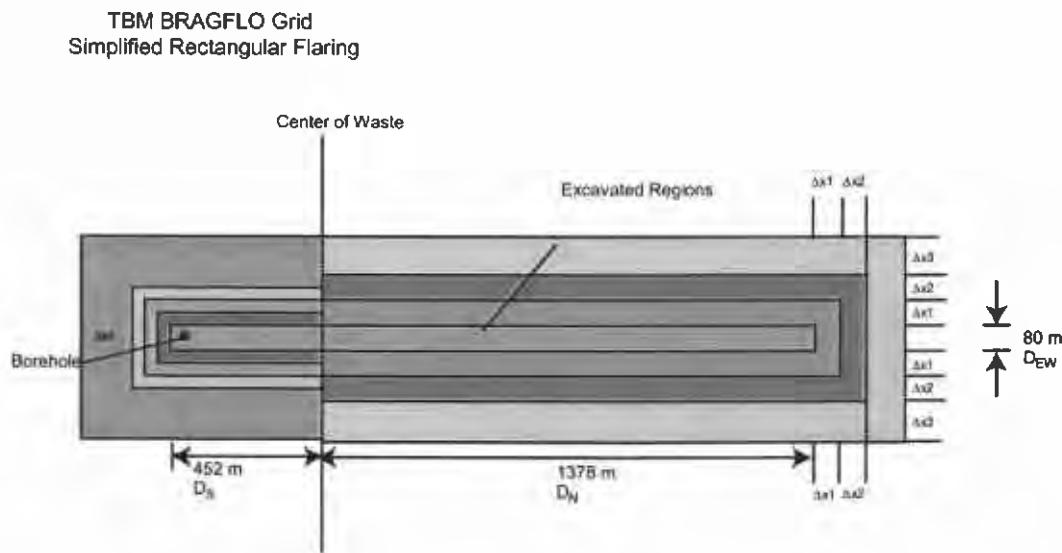
$$\Delta z_3 = 2D_N + D_{EW} + 4\Delta x_1 + 4\Delta x_2 + 2\Delta x_3$$

$$\Delta z_n = 2D_N + D_{EW} + 4 \sum_{i=1}^{n-1} \Delta x_i + 2\Delta x_n$$

Flaring for blocks wrapped around the southern end is the same with D_S substituted for D_N .

This method of rectangular flaring ensures that the grid accounts for all the volume surrounding the repository.

Figure 4.



2.5 Refinement of the X-spacing outside the repository.

The grid blocks to the north and south of the excavated region will be refined in the x -direction from the baseline grid. The x -dimension of the grid cells immediately to the north and south of the repository start at 2 m and increases by a factor of 1.45. Exceptions to this are made to ensure that the location of the Land Withdrawal Boundary and the total extent of the grid matches that in the baseline grid. This refinement factor was chosen to reduce numerical dispersion caused by rapid increases in cell dimensions (Anderson and Woessner, 1992; Wang and Anderson, 1982).

2.6 Refinement of the Y-spacing.

In the y -direction the grid spacing within layers representing the Salado has been changed from the baseline. The CCA grid spacing in the Salado was dictated by the thickness of different shaft seal materials. Since the shaft is longer represented in the model domain, the y spacing in the Salado is now uniform. In addition, two layers were added immediately above and below Marker Bed 139 to refine the grid spacing and reduce numerical dispersion. These changes result in a total of 33 y -divisions for the grid, and will increase the accuracy of flow and transport calculations.

3.0 LOGICAL GRIDS

Figure 5.

Baseline Grid

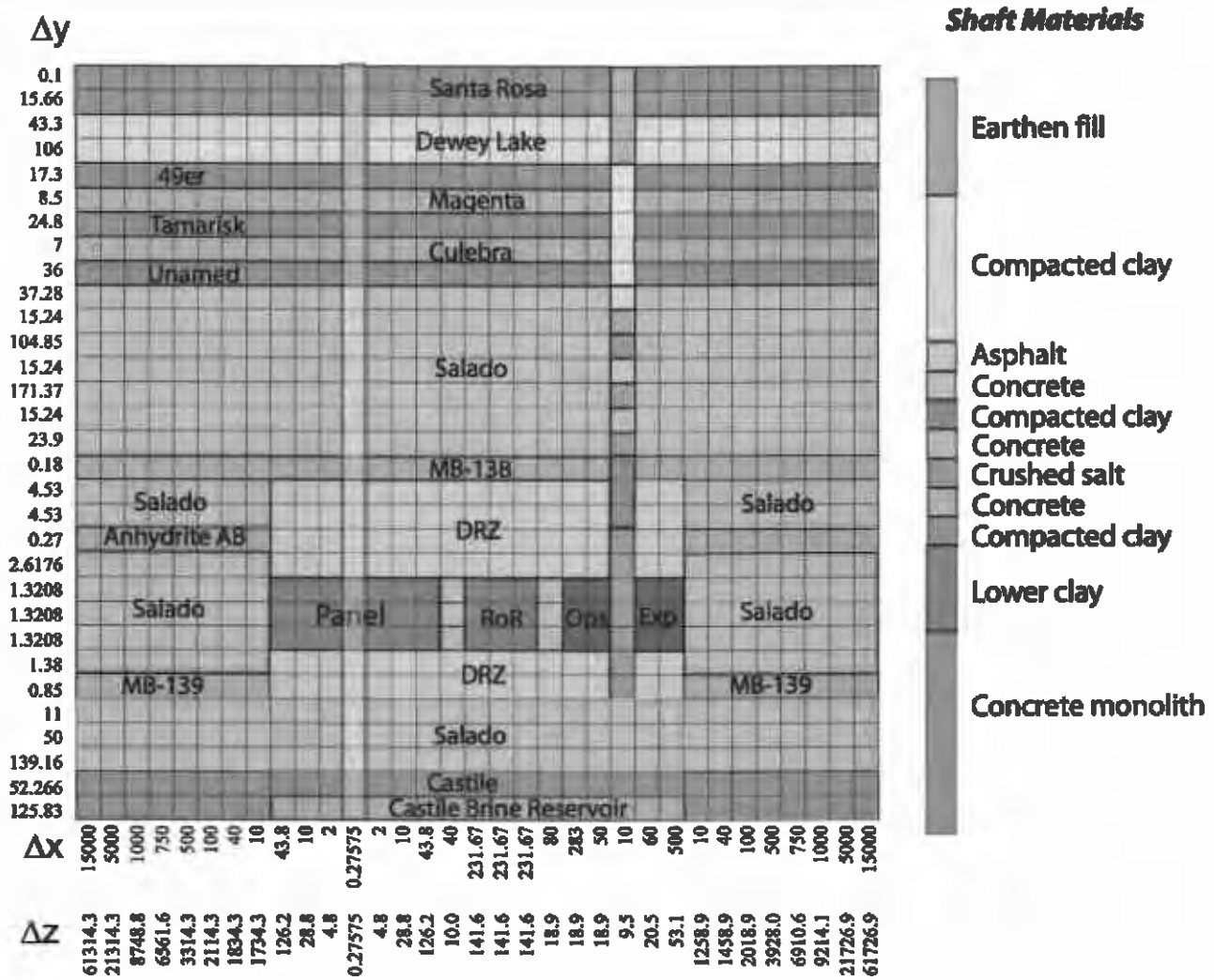
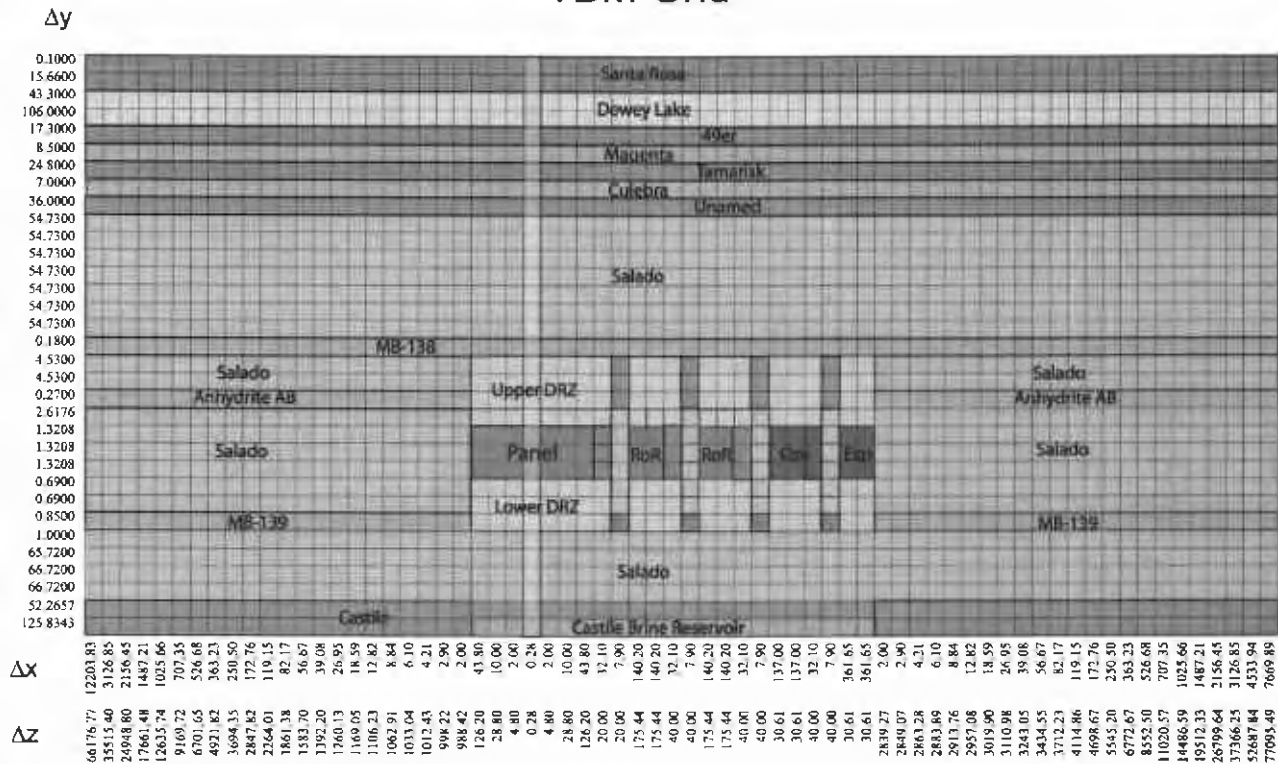


Figure 6.

TBM Grid



3.0 GRID CALCULATIONS

Attached to this memo is an Excel Spreadsheet entitled “TBM_Grid_Dimensions_5-2002a.xls” that calculates grid dimensions that are fed into GENMESH to make the TBM BRAGFLO grid. The key information that GENMESH needs for input is ΔX and ΔZ for each grid column and ΔY for each grid row. These values are listed in Excel columns labeled, “del X”, “del Z”, and “del Y”. Parameters used for the flaring calculation are grouped together under the heading “Flaring Parameters”. The volume of grid cells in the repository is listed because it is used to calculate the flaring parameters.

4.0 REFERENCES

Anderson, M.P., Woessner, W.W., 1992, Applied Groundwater Modeling: Simulation of Flow and Advective Transport, Academic Press, Inc.

Helton et al., 1998, Uncertainty and Sensitivity Analysis Results Obtained in the 1996 Performance Assessment for the Waste Isolation Pilot Plant, SAND98-0365.

PAVT, 1997, Supplemental Summary of EPA-Mandated Performance Assessment Verification Test (All Replicates) and Comparison with the Compliance Certification Application Calculations, WPO# 46702, Report # 414879.

Stein, J.S., 2002, Analysis Plan for Calculations of Salado Flow: Technical Baseline Migration (TBM), AP-086.

U.S. DOE (U.S. Department of Energy), 1996, Title 40 CRF Part 191 Compliance Certification Application for the Waste Isolation Pilot Plant. DOE/CAO-1996-2184.

Wang, H.F, Anderson, M.P., 1982, Introduction to Groundwater Modeling: Finite Difference and Finite Element Methods, Academic Press, Inc.

	A	B	C	D	E	F
1	Spreadsheet to calculate the TBM grid dimensions for input into GENMESH					
2	Developed by Joshua S. Stein, Ph. D.					
3	Sandia National Laboratories, Carlsbad, NM					
4						
5		Flaring Parameters		grid-waste offset=	462.71	
6		Dn	1377.7	Excavation length=	1829.98	
7		Dew	79.87	Excavation volume=	579153.92	
8		Ds	452.28	Excavation volume=	579153.92	
9		refine factor	1.45			
10		SOUTH				
11	Column Index	del X	del Z	Volume in Rep	Row Index	del V
12	1	12203.83	66176.78		1	125.8343
13	2	3126.85	35515.41		2	52.2657
14	3	2156.45	24948.80		3	66.7200
15	4	1487.21	17661.49		4	66.7200
16	5	1025.66	12635.75		5	65.7200
17	6	707.35	9169.73		6	1.0000
18	7	526.68	6701.66		7	0.8500
19	8	363.23	4921.83		8	0.6900
20	9	250.50	3694.36		9	0.6900
21	10	172.76	2847.83		10	1.3208
22	11	119.15	2264.02		11	1.3208
23	12	82.17	1861.39		12	1.3208
24	13	56.67	1583.71		13	2.6176
25	14	39.08	1392.21		14	0.2700
26	15	26.95	1260.14		15	4.5300
27	16	18.59	1169.06		16	4.5300
28	17	12.82	1106.24		17	0.1800
29	18	8.84	1062.92		18	54.7300
30	19	6.10	1033.05		19	54.7300
31	20	4.21	1012.44		20	54.7300
32	21	2.90	998.23		21	54.7300
33	22	2.00	988.43		22	54.7300
34	23	43.80	126.20	21902.40374	23	54.7300
35	24	10.00	28.80	1141.1712	24	54.7300
36	25	2.00	4.80	38.03904	25	36.0000

	A	B	C	D	E	F
37	26	0.28	0.28	0.31065216	26	7.0000
38	27	2.00	4.80	38.03904	27	24.8000
39	28	10.00	28.80	1141.1712	28	8.5000
40	29	43.80	126.20	21902.40374	29	17.3000
41	30	32.10	20.00	2543.8608	30	106.0000
42	31	7.90	20.00	626.0592	31	43.3000
43	32	140.20	175.44	97459.83847	32	15.6600
44	33	140.20	175.44	97459.83847	33	0.1000
45	34	32.10	40.00	5087.7216		
46	35	7.90	40.00	1252.1184		
47	36	140.20	175.44	97459.83847		
48	37	140.20	175.44	97459.83847		
49	38	32.10	40.00	5087.7216		
50	39	7.90	40.00	1252.1184		
51	40	137.00	30.61	16616.60177		
52	41	137.00	30.61	16616.60177		
53	42	32.10	40.00	5087.7216		
54	43	7.90	40.00	1252.1184		
55	44	361.65	30.61	43864.19		
56	45	361.65	30.61	43864.19		
57	46	2.00	2839.27			
58	47	2.90	2849.07			
59	48	4.21	2863.28			
60	49	6.10	2883.89			
61	50	8.84	2913.76			
62	51	12.82	2957.08			
63	52	18.59	3019.90			
64	53	26.95	3110.98			
65	54	39.08	3243.05			
66	55	56.67	3434.55			
67	56	82.17	3712.23			
68	57	119.15	4114.86			
69	58	172.76	4698.67			
70	59	250.50	5545.20			
71	60	363.23	6772.67			
72	61	526.68	8552.50			

	A	B	C	D	E	F
73	62	707.35	11020.57			
74	63	1025.66	14486.59			
75	64	1487.21	19512.33			
76	65	2156.45	26799.64			
77	66	3126.85	37366.25			
78	67	4533.94	52687.84			
79	68	7669.89	77095.49			
80		NORTH				
81						

	A	B
1	<i>Spreadsheet to calculate the TBM grid dimensions for input into GENMESH</i>	
2	<i>Developed by Joshua S. Stein, Ph. D.</i>	
3	<i>Sandia National Laboratories, Carlsbad, NM</i>	
4		
5		Flaring Parameters
6		Dn
7		Dew
8		Ds
9		refine factor
10		SOUTH
11	Column Index	del X
12	1	12203.828
13	=A12+1	=B14*\$C\$9
14	=A13+1	=B15*\$C\$9
15	=A14+1	=B16*\$C\$9
16	=A15+1	=B17*\$C\$9
17	=A16+1	=B18*\$C\$9-56.3397
18	=A17+1	=B19*\$C\$9
19	=A18+1	=B20*\$C\$9
20	=A19+1	=B21*\$C\$9
21	=A20+1	=B22*\$C\$9
22	=A21+1	=B23*\$C\$9
23	=A22+1	=B24*\$C\$9
24	=A23+1	=B25*\$C\$9
25	=A24+1	=B26*\$C\$9
26	=A25+1	=B27*\$C\$9
27	=A26+1	=B28*\$C\$9
28	=A27+1	=B29*\$C\$9
29	=A28+1	=B30*\$C\$9
30	=A29+1	=B31*\$C\$9
31	=A30+1	=B32*\$C\$9
32	=A31+1	=B33*\$C\$9
33	=A32+1	2
34	=A33+1	43.8
35	=A34+1	10
36	=A35+1	2

	A	B
37	=A36+1	0.28
38	=A37+1	2
39	=A38+1	10
40	=A39+1	43.8
41	=A40+1	32.1
42	=A41+1	7.9
43	=A42+1	=280.4/2
44	=A43+1	=280.4/2
45	=A44+1	32.1
46	=A45+1	7.9
47	=A46+1	=280.4/2
48	=A47+1	=280.4/2
49	=A48+1	32.1
50	=A49+1	7.9
51	=A50+1	=274/2
52	=A51+1	=274/2
53	=A52+1	32.1
54	=A53+1	7.9
55	=A54+1	361.65
56	=A55+1	361.65
57	=A56+1	2
58	=A57+1	=B57*\$C\$9
59	=A58+1	=B58*\$C\$9
60	=A59+1	=B59*\$C\$9
61	=A60+1	=B60*\$C\$9
62	=A61+1	=B61*\$C\$9
63	=A62+1	=B62*\$C\$9
64	=A63+1	=B63*\$C\$9
65	=A64+1	=B64*\$C\$9
66	=A65+1	=B65*\$C\$9
67	=A66+1	=B66*\$C\$9
68	=A67+1	=B67*\$C\$9
69	=A68+1	=B68*\$C\$9
70	=A69+1	=B69*\$C\$9
71	=A70+1	=B70*\$C\$9
72	=A71+1	=B71*\$C\$9

	A	B
73	=A72+1	=B72*\$C\$9-56.3397
74	=A73+1	=B73*\$C\$9
75	=A74+1	=B74*\$C\$9
76	=A75+1	=B75*\$C\$9
77	=A76+1	=B76*\$C\$9
78	=A77+1	=B77*\$C\$9
79	=A78+1	7669.89
80		NORTH
81		

	C	D	E	F
1				
2				
3				
4				
5		grid-waste offset=	=C6-E6/2	
6	=SUM(B47:B56)+(B46+B45)/2	Excavation length=	=SUM(B34:B56)	
7	=E7/E6/3.9624	Excavation volume=	=SUM(D34:D56)	
8	=SUM(B34:B44)+(B46+B45)/2	Excavation volume=	=(C6+C8)*C7*3.9624	
9	L45			
10				
11	del Z	Volume in Rep	Row Index	del Y
12	=2*\$C\$8)+(\$C\$7)+(4*SUM(B13:B\$33)))+(2*B12		1	125.8343
13	=2*\$C\$8)+(\$C\$7)+(4*SUM(B14:B\$33)))+(2*B13		=E12+1	52.2657
14	=2*\$C\$8)+(\$C\$7)+(4*SUM(B15:B\$33)))+(2*B14		=E13+1	66.72
15	=2*\$C\$8)+(\$C\$7)+(4*SUM(B16:B\$33)))+(2*B15		=E14+1	66.72
16	=2*\$C\$8)+(\$C\$7)+(4*SUM(B17:B\$33)))+(2*B16		=E15+1	65.72
17	=2*\$C\$8)+(\$C\$7)+(4*SUM(B18:B\$33)))+(2*B17		=E16+1	1
18	=2*\$C\$8)+(\$C\$7)+(4*SUM(B19:B\$33)))+(2*B18		=E17+1	0.85
19	=2*\$C\$8)+(\$C\$7)+(4*SUM(B20:B\$33)))+(2*B19		=E18+1	=1.38/2
20	=2*\$C\$8)+(\$C\$7)+(4*SUM(B21:B\$33)))+(2*B20		=E19+1	=1.38/2
21	=2*\$C\$8)+(\$C\$7)+(4*SUM(B22:B\$33)))+(2*B21		=E20+1	1.3208
22	=2*\$C\$8)+(\$C\$7)+(4*SUM(B23:B\$33)))+(2*B22		=E21+1	1.3208
23	=2*\$C\$8)+(\$C\$7)+(4*SUM(B24:B\$33)))+(2*B23		=E22+1	1.3208
24	=2*\$C\$8)+(\$C\$7)+(4*SUM(B25:B\$33)))+(2*B24		=E23+1	2.6176
25	=2*\$C\$8)+(\$C\$7)+(4*SUM(B26:B\$33)))+(2*B25		=E24+1	0.27
26	=2*\$C\$8)+(\$C\$7)+(4*SUM(B27:B\$33)))+(2*B26		=E25+1	4.53
27	=2*\$C\$8)+(\$C\$7)+(4*SUM(B28:B\$33)))+(2*B27		=E26+1	4.53
28	=2*\$C\$8)+(\$C\$7)+(4*SUM(B29:B\$33)))+(2*B28		=E27+1	0.18
29	=2*\$C\$8)+(\$C\$7)+(4*SUM(B30:B\$33)))+(2*B29		=E28+1	54.73
30	=2*\$C\$8)+(\$C\$7)+(4*SUM(B31:B\$33)))+(2*B30		=E29+1	54.73
31	=2*\$C\$8)+(\$C\$7)+(4*SUM(B32:B\$33)))+(2*B31		=E30+1	54.73
32	=2*\$C\$8)+(\$C\$7)+(4*B33)+(2*B32)		=E31+1	54.73
33	=2*\$C\$8)+(\$C\$7)+(2*\$B33)		=E32+1	54.73
34	126.2	=B34*C34*3.9624	=E33+1	54.73
35	28.8	=B35*C35*3.9624	=E34+1	54.73
36	4.8	=B36*C36*3.9624	=E35+1	36

	C	D	E	F
37	0.28	=B37*C37*3.9624	=E36+1	7
38	4.8	=B38*C38*3.9624	=E37+1	24.8
39	28.8	=B39*C39*3.9624	=E38+1	8.5
40	126.2	=B40*C40*3.9624	=E39+1	17.3
41	20	=B41*C41*3.9624	=E40+1	106
42	20	=B42*C42*3.9624	=E41+1	43.3
43	175.436259299742	=B43*C43*3.9624	=E42+1	15.66
44	175.436259299742	=B44*C44*3.9624	=E43+1	0.1
45	40	=B45*C45*3.9624		
46	40	=B46*C46*3.9624		
47	175.436259299742	=B47*C47*3.9624		
48	175.436259299742	=B48*C48*3.9624		
49	40	=B49*C49*3.9624		
50	40	=B50*C50*3.9624		
51	30.61	=B51*C51*3.9624		
52	30.61	=B52*C52*3.9624		
53	40	=B53*C53*3.9624		
54	40	=B54*C54*3.9624		
55	30.61	=B55*C55*3.9624		
56	30.61	=B56*C56*3.9624		
57	= (2*\$C\$6)+(\$C\$7)+(2*\$B57)			
58	= (2*\$C\$6)+(\$C\$7)+(4*\$B57)+(2*\$B58)			
59	= (2*\$C\$6)+(\$C\$7)+(4*SUM(B\$57:B58))+ (2*\$B59)			
60	= (2*\$C\$6)+(\$C\$7)+(4*SUM(B\$57:B59))+ (2*\$B60)			
61	= (2*\$C\$6)+(\$C\$7)+(4*SUM(B\$57:B60))+ (2*\$B61)			
62	= (2*\$C\$6)+(\$C\$7)+(4*SUM(B\$57:B61))+ (2*\$B62)			
63	= (2*\$C\$6)+(\$C\$7)+(4*SUM(B\$57:B62))+ (2*\$B63)			
64	= (2*\$C\$6)+(\$C\$7)+(4*SUM(B\$57:B63))+ (2*\$B64)			
65	= (2*\$C\$6)+(\$C\$7)+(4*SUM(B\$57:B64))+ (2*\$B65)			
66	= (2*\$C\$6)+(\$C\$7)+(4*SUM(B\$57:B65))+ (2*\$B66)			
67	= (2*\$C\$6)+(\$C\$7)+(4*SUM(B\$57:B66))+ (2*\$B67)			
68	= (2*\$C\$6)+(\$C\$7)+(4*SUM(B\$57:B67))+ (2*\$B68)			
69	= (2*\$C\$6)+(\$C\$7)+(4*SUM(B\$57:B68))+ (2*\$B69)			
70	= (2*\$C\$6)+(\$C\$7)+(4*SUM(B\$57:B69))+ (2*\$B70)			
71	= (2*\$C\$6)+(\$C\$7)+(4*SUM(B\$57:B70))+ (2*\$B71)			
72	= (2*\$C\$6)+(\$C\$7)+(4*SUM(B\$57:B71))+ (2*\$B72)			

	C	D	E	F
73	=(2*\$C\$6)+(\$C\$7)+(4*SUM(B\$57:B72))+(2*B73)			
74	=(2*\$C\$6)+(\$C\$7)+(4*SUM(B\$57:B73))+(2*B74)			
75	=(2*\$C\$6)+(\$C\$7)+(4*SUM(B\$57:B74))+(2*B75)			
76	=(2*\$C\$6)+(\$C\$7)+(4*SUM(B\$57:B75))+(2*B76)			
77	=(2*\$C\$6)+(\$C\$7)+(4*SUM(B\$57:B76))+(2*B77)			
78	=(2*\$C\$6)+(\$C\$7)+(4*SUM(B\$57:B77))+(2*B78)			
79	=(2*\$C\$6)+(\$C\$7)+(4*SUM(B\$57:B78))+(2*B79)			
80				
81				